

## Diffuse and streamer regions of sprites

Victor P. Pasko

CSSL Laboratory, Penn State University, University Park, Pennsylvania, USA

Hans C. Stenbaek-Nielsen

Geophysical Institute, University of Alaska Fairbanks, Alaska, USA

Received 25 October 2001; revised 9 November 2001; accepted 3 December 2001; published 28 May 2002.

[1] The observed altitude stratification in large number of sprite events, exhibiting a sharp transition between the upper diffuse and lower streamer regions, is used in conjunction with a theoretical model to establish correspondence between sprite luminosity and the ambient mesospheric/lower ionospheric conductivity profile. The reported results provide new means for remote sensing of the lower ionosphere using sprite luminosity. *INDEX TERMS:* 2427 Ionosphere: Ionosphere/atmosphere interactions (0335); 3304 Meteorology and Atmospheric Dynamics: Atmospheric electricity; 3324 Meteorology and Atmospheric Dynamics: Lightning

### 1. Introduction

[2] Sprites are spectacular luminous features which occur at mesospheric/lower ionospheric altitudes above lightning storms [e.g., *Sentman et al.*, 1995]. Individual sprites can be large covering altitudes from about 30 km to 100 km with a diameter of up to almost 100 km [e.g., *Stenbaek-Nielsen et al.*, 2000]. The theoretical analysis of *Pasko et al.* [1998a] indicates existence of three distinct altitude regions in sprites: (1) The upper diffuse region; (2) The intermediate transition region; (3) The lower streamer region (Figure 1a). Sprites indeed often exhibit an amorphous non structured glow at their tops which converts to highly structured (predominantly vertical) breakdown regions at lower altitudes [e.g., *Stanley et al.*, 1999; *Gerken et al.*, 2000; *Barrington-Leigh et al.*, 2001a; *Wescott et al.*, 2001]. This vertical structuring in sprites is especially apparent in the recent high speed video images of *Stenbaek-Nielsen et al.* [2000], which allow to identify a quite sharp transition between the diffuse and streamer regions as apparent in Figures 1b, 2a, and 2b.

[3] The unique feature of the sprite imaging data reported by *Stenbaek-Nielsen et al.* [2000] is that all observations were consistently performed with full gain of the intensified CCD imager. As a result most, if not all, sprite events substantially saturated the imager at onset. However, subsequent frames provided unprecedented recordings of temporal development of low light sprite features. In particular, most of the recorded events show in considerable detail the transition between the upper diffuse and the lower streamer regions of sprites discussed in [*Pasko et al.*, 1998a].

[4] Although it has been fully realized since early sprite observations that their upper termination is closely associated with the lower ledge of the ionospheric D-region electron density profile [e.g., *Sentman et al.*, 1995], the observed vertical sprite structuring (Figure 1b) is generally a more complicated effect which can be characterized by interplay and sharp altitude variation of at least three physical parameters (the dissociative attachment time scale  $\tau_a$ , the ambient dielectric relaxation time scale  $\tau_\sigma$  and the time for the development of an individual electron avalanche into a

streamer  $t_s$ ) [*Pasko et al.*, 1998a]. These parameters effectively carry information about the internal physics of the sprite electrical breakdown (i.e., the ionization and attachment rates) as well as the state of the ambient ionosphere (i.e., the electron density profile). It therefore becomes attractive to use the observed vertical structuring in sprites to test the basic concepts of the proposed sprite mechanisms (i.e., the streamer type conventional breakdown) as well as to extract information about the ambient lower ionospheric conditions. The purpose of this paper is to undertake a first simple study of this sort. Analyzing the transition region, as identified in the high speed imager data, we can place bounds on the mesospheric/lower ionospheric conductivity profiles available in the literature.

### 2. Observed Altitude Stratification in Sprites

[5] For the present study we use the data set of sprite events recorded by *Stenbaek-Nielsen et al.* [2000] over southeastern Nebraska during three hour time period between 4 and 7 UT on August 18, 1999. Although the observed events are generally complex in terms of their temporal dynamics and spatial features [*Stenbaek-Nielsen et al.*, 2000] most of the events allowed a simple definition of the horizontal boundary, which separates the diffuse and streamer regions of sprites (Figure 2). The total of 25 events has been analyzed in this way and the corresponding altitude of the transition has been recorded assuming that sprite is centered right above the causative lightning discharge. The uncertainty introduced by this assumption is discussed below. The coordinates of the causative lightning discharges were provided by the National Lightning Detection Network (NLDN).

[6] Figure 3a gives a summary of all 25 measurements as a function of time (in minutes after 4 UT on August 18, 1999). The solid line shows the least squares linear fit to the data points and the horizontal dashed line shows the mean value. Figure 3b provides a histogram demonstrating frequency of occurrence of events at different altitudes. The mean transition altitude appears to be 78.2 km with the standard deviation 4.0 km. The minimum observed transition altitude is 70.6 km and the maximum is 87.0 km. The histogram in Figure 3b has a shape close to Gaussian. The slight (several km) increase in the transition altitude as a function of time shown in Figure 3a by the least squares linear fit is not statistically important since it is comparable to the standard deviation. Nevertheless this may represent a trace of the changing ambient electron density profile during the night. The calculations with the International Reference Ionosphere (IRI-95) model indicate that there is approximately 1 km shift (upward) of the electron density profile between 4 UT and 7 UT as illustrated in Figure 4b by profiles 4 and 5.

[7] It is well known that sprites are often not centered right above the causative lightning discharges [e.g., *Lyons*, 1996; *Wescott et al.*, 2001]. *Wescott et al.* [2001] report a mean horizontal distance relative to the associated NLDN strikes of 25.2 km. Applying this value to our set of 25 events results in a mean altitude shift of  $\pm 4.4$  km. The standard deviation in our altitude

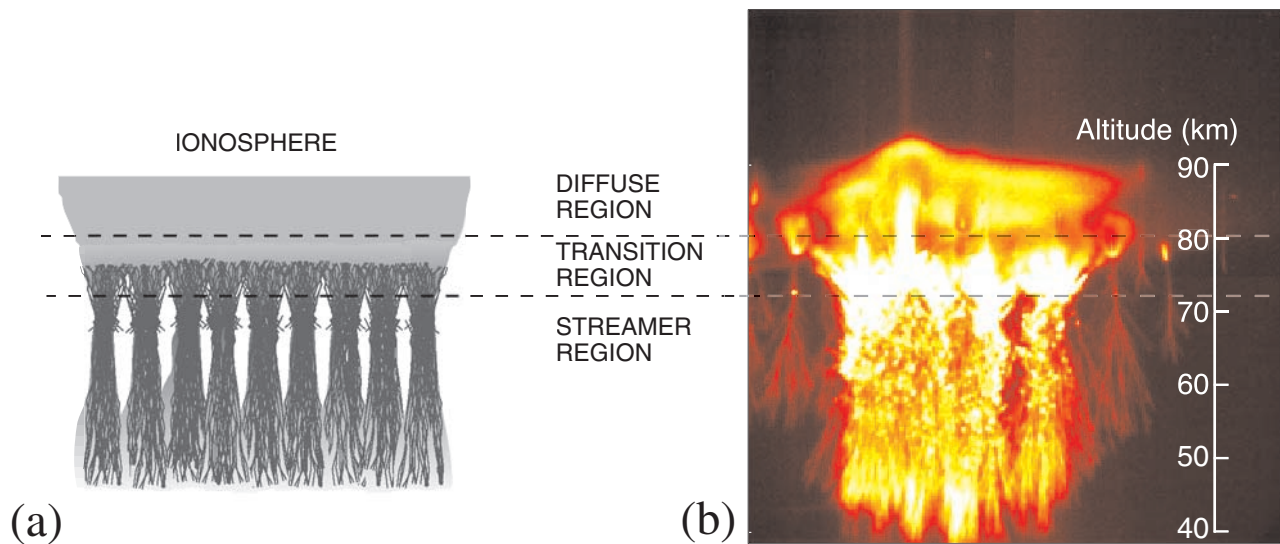


**Figure 1.** The vertical altitude structuring in sprites. (a) The proposed theoretical model [Pasko *et al.*, 1998a, 1998b]; (b) Results of video observations [Stenbaek-Nielsen *et al.*, 2000]. The original black and white image from [Stenbaek-Nielsen *et al.*, 2000] is reproduced in false color.

measurement, assuming the sprites at the NLDN strike, is also  $\sim 4$  km (Figure 3b). Hence, it is reasonable to assume that the observed spread of the altitude points in Figure 3 is primarily due to the uncertainty in the location of the sprites. The examples shown in Figure 2 have very similar features, which reasonably would be expected to be at similar altitudes. A few, currently unpublished [E. M. Wescott, private communication, 2001], triangulated sprite features at or near the transition also support this assumption. We therefore adopt the hypothesis that the mean transition altitude in Figure 3a (78.2 km) is the true transition

altitude for all observed events. At the same time we emphasize that although we adopt this hypothesis as reasonable, the available information does not allow us to conclusively prove it.

### 3. Sprite Structure as a Measure of the Lower Ionosphere

[8] We now investigate how the transition altitude measurements provided in Figure 3 can be related to the ambient night time

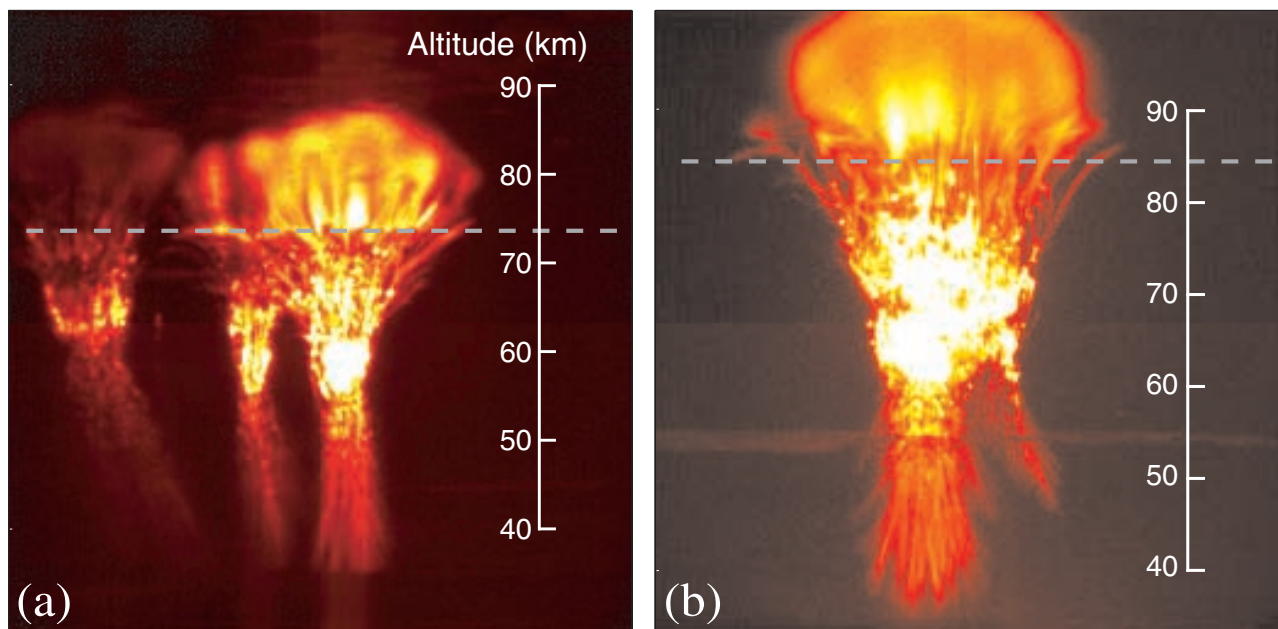


**Figure 2.** The images illustrating the altitude transition between diffuse and streamer regions in sprites observed on August 18, 1999 by Stenbaek-Nielsen *et al.* [2000]. The times given are those of the associated NLDN event. (a) 04:36:09.230 UT; (b) 05:24:22.804 UT. The original black and white images from [Stenbaek-Nielsen *et al.*, 2000] are reproduced in false color.

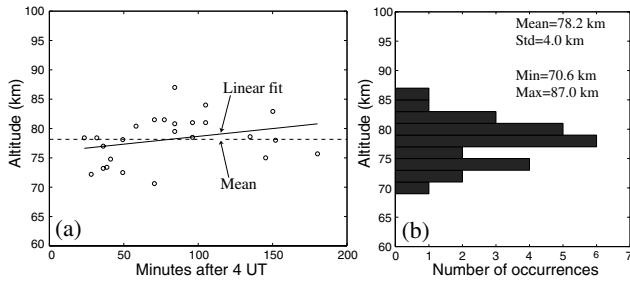


**Figure 3.** Results of the experimental measurements of the transition altitude in 25 sprites as a function of time (a), and in a histogram form showing number of occurrences as a function of altitude (b).

ionospheric conditions. For our study we use three model ion conductivity profiles (Figure 4a) and five model electron density profiles (Figure 4b). The ion Profile A (Figure 4a) represents a summary of rocket measurements at night at mid latitudes from [Hale, 1994]. Profile B is taken from [Park and Dejnarintra, 1973, Figure 4c, and Dejnarintra and Park, 1974, Figure 4a]. Profile C is derived from results of balloon and rocket measurements above active thunderstorms [Holzworth et al., 1985]. The five electron number density profiles are shown in Figure 4b. Profile 1 is from [Wait and Spies, 1964; Inan, 1990]. Profile 2 is from [Reagan et al., 1981] and Profile 3 is from [Hale, 1994]. Profiles 4 and 5 for the altitude range above 80 km are from the International Reference Ionosphere (IRI-95) Model (<http://nssdc.gsfc.nasa.gov/space/model/models/iri.html>) for 4 UT and 7 UT respectively, on 18 August 1999 at 40.42N and 261.19E. The information about nighttime electron density below 80 km is not available from the IRI model and for altitudes <80 km we assumed these profiles to be the same as the model Profile 3.

[9] The above profiles combine to a total of 15 model conductivity profiles. Each profile ( $\sigma$ ) is constructed by adding an ion conductivity from Figure 4a to the electron conductivity derived from one of the electron density profiles in Figure 4b. The electron conductivity is calculated as  $en_e\mu_e$ , where  $n_e$  is the electron number density,  $e$  the electron charge, and  $\mu_e = 0.044 N_o/N$  m<sup>2</sup>/V/s the electron mobility.  $N$  is the altitude dependent atmospheric neutral density and  $N_o$  is its value at ground level [Pasko et al., 1997 and references therein]. Figure 5a illustrates the theoretical approach proposed by Pasko et al. [1998a] to identify the transition region boundaries. We use this to analyze the 15 model ambient conductivity profiles. Following Pasko et al. [1998a] it is assumed that the observed vertical structuring in sprites is created due to interplay of three physical time scales: (1) The dissociative attachment time scale  $\tau_a$  (which is defined by the maximum net attachment coefficient as  $1/(v_a - v_i)_{\max}$ , where  $v_i$  and  $v_a$  are the ionization and attachment coefficients, respectively); (2) The ambient dielectric

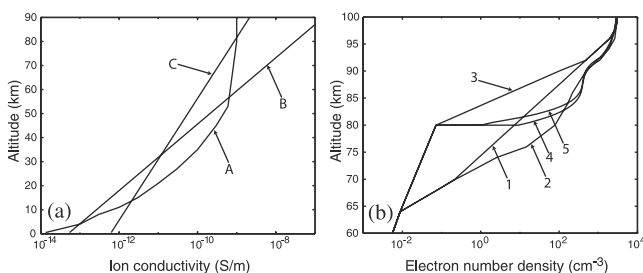


**Figure 4.** Model altitude profiles of (a) ion conductivity, and (b) ambient electron density used in the analysis.

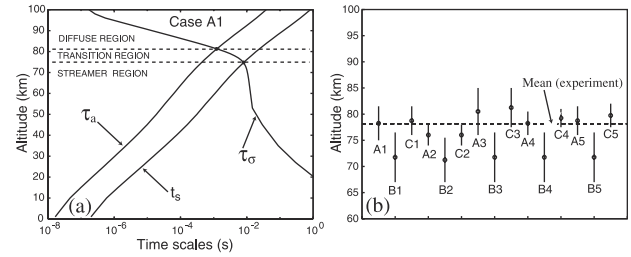


**Figure 5.** (a) The altitude distribution of different time scales characterizing the electrical breakdown associated with sprites [Pasko et al., 1998a]. (b) The comparison of the experimental data (horizontal dashed line) and theoretical results for different ambient conductivity profiles.

relaxation time scale  $\tau_\sigma = \epsilon_0/\sigma$  (shown in Figure 5a for the model case A1, i.e., the ion conductivity Profile A and electron number density Profile 1); (3) The time scale for the development of an individual electron avalanche into a streamer  $t_s$  (this is an effective time over which the avalanche generates a space charge field comparable in magnitude to the externally applied field [e.g., Pasko et al., 1998a]). The altitude distribution of  $\tau_a$  in Figure 5a uses the updated ionization and attachment coefficients given by [Barrington-Leigh et al., 2001b]. For calculation of  $t_s$  we assume the external electric field to be 10% above the breakdown threshold level  $E_k = 3.23 \times 10^6 N_o/N$  (defined as the field value at which  $v_i = v_a$ ). The interplay between these three parameters creates three unique altitude regions as illustrated in Figure 5a: (1) The diffuse region ( $\tau_\sigma < \tau_a$ ,  $\tau_\sigma < t_s$ ) characterized by collective multiplication of electrons (Townsend mechanism); (2) The transition region ( $\tau_\sigma > \tau_a$ ,  $\tau_\sigma < t_s$ ) characterized by strong attachment of ambient electrons before the onset of the electrical breakdown; (3) The streamer region ( $\tau_\sigma > \tau_a$ ,  $\tau_\sigma > t_s$ ) also characterized by the strong attachment as well as by individual electron avalanches evolving into streamers. The upper and the lower boundaries of the transition region shown in Figure 5a represent an estimate of the altitude range in which the actual transition between the diffuse and streamer regions is expected to occur. The upper boundary may shift downward under conditions of an impulsive lightning discharge which generates substantial electron density (i.e., conductivity) enhancement associated with the sprite halo at the initial stage of sprite formation [e.g., Barrington-Leigh et al., 2001a]. The lower boundary may shift upward due to streamers originating at lower altitudes but propagating upward toward the lower ionosphere [e.g., Stanley et al., 1999]. For our comparison with experimental data (Figure 5b) we use the full transition altitude range, i.e., between intersections of  $\tau_\sigma$  and  $t_s$  curves, and  $\tau_\sigma$  and  $\tau_a$  curves in Figure 5a. The open circles are the intermediate altitude points and the vertical lines are the full theoretical transition altitude range.

[10] Based on the comparison between experimental measurements and theory (Figure 5b) some ambient conductivity profiles can be discarded. For example, all combinations involving the ion profile B and electron profiles 2 and 3 can be eliminated since they do not fit the experimental measurements of the transition altitude well. In this context we note that Profile B was used in the original sprite model by Pasko et al. [1995] leading to quite high charge values to be removed by lightning ( $\sim 100$  C from 10 km altitude) in order to produce visible sprites. From this point of view profiles A and C are more realistic and the video data analyzed here support them. The electron profile 1 based on the D-region model of Wait and Spies [1964] and Inan [1990] (which also has been successfully used in recent modeling of sprite halos by Barrington-Leigh et al. [2001a]), and both IRI profiles agree with the analyzed video data very well. It is important to emphasize that our analysis only allows remote sensing of the conductivity profile in the altitude region of

the observed transition (around  $\sim 80$  km) and does not provide means to extract information about the entire altitude profiles.

#### 4. Summary

[11] We have evaluated the transition boundary between the diffuse and streamer regions of sprites by comparing model results of [Pasko *et al.*, 1998a] with images recorded at 1000 frames per second [Stenbaek-Nielsen *et al.*, 2000]. Analysis of 25 events indicate a mean transition altitude of 78.2 km with a standard deviation of 4.0 km. A part of this standard deviation must be due to the well-established fact that sprites do not occur exactly over the lightning strike as assumed in our analysis. Wescott *et al.* [2001] report a mean 25.2 km between the NLDN strike location and the sprite, and applying this uncertainty to our data set leads to a similar standard deviation. This indicates that most, if not all, of the spread in transition altitude may be due to uncertainty in sprite location and not true variations in transition altitude. Thus, it seems reasonable to argue that the transition altitude actually varies little over the 3 hours of observations used in the study. The transition altitude is a sensitive function of the ambient parameters at the mesospheric and lower ionospheric altitudes (i.e., the electron number density profile). Hence, our measurements can be used to evaluate model profiles of the ambient conductivity at sprite altitudes compiled from existing models and literature on this subject. For the electron density profiles, in particular, the best fit between the model and observations is for profiles calculated using the IRI-95 model and the night time electron density profile by Wait and Spies [1964] (see also Inan, 1990). This profile also produced the best fit between the high speed video observations of sprite halos and model results reported recently by Barrington-Leigh *et al.* [2001a].

[12] **Acknowledgments.** This research was supported by the Electrical Engineering Department of Penn State University and State of Alaska research support to the Geophysical Institute, University of Alaska Fairbanks.

#### References

- Barrington-Leigh, C. P., U. S. Inan, and M. Stanley, Identification of sprites and elves with intensified video and broadband array photometry, *J. Geophys. Res.*, *106*, 1741, 2001a.
- Barrington-Leigh, C. P., V. P. Pasko, and U. S. Inan, Exponential relaxation of optical emissions in sprites, *J. Geophys. Res.*, *106*, in press, 2001b.
- Dejnakarintra, M., and C. G. Park, Lightning-induced electric fields in the ionosphere, *J. Geophys. Res.*, *79*, 1903, 1974.
- Gerken, E. A., U. S. Inan, and C. P. Barrington-Leigh, Telescopic imaging of sprites, *Geophys. Res. Lett.*, *27*, 2637, 2000.
- Hale, L. C., Coupling of ELF/ULF energy from lightning and MeV particles to the middle atmosphere, ionosphere, and global circuit, *J. Geophys. Res.*, *99*, 21,089, 1994.
- Holzworth, R. H., M. C. Kelley, C. L. Siefring, L. C. Hale, and J. T. Mitchell, Electrical measurements in the atmosphere and the ionosphere over an active thunderstorm. 2. Direct current electric fields and conductivity, *J. Geophys. Res.*, *90*, 9824, 1985.
- Inan, U. S., VLF heating of the lower ionosphere, *Geophys. Res. Lett.*, *17*, 729, 1990.
- Lyons, W. A., Sprite observations above the U. S. High Plains in relation to their parent thunderstorm systems, *J. Geophys. Res.*, *101*, 29,641, 1996.
- Park, C. G., and M. Dejnakarintra, Penetration of thundercloud electric fields into the ionosphere and magnetosphere. 1. Middle and subauroral latitudes, *J. Geophys. Res.*, *78*, 6623, 1973.
- Pasko, V. P., U. S. Inan, Y. N. Taranenko, and T. F. Bell, Heating, ionization and upward discharges in the mesosphere due to intense quasi-electrostatic thundercloud fields, *Geophys. Res. Lett.*, *22*, 365, 1995.
- Pasko, V. P., U. S. Inan, T. F. Bell, and Y. N. Taranenko, Sprites produced by quasi-electrostatic heating and ionization in the lower ionosphere, *J. Geophys. Res.*, *102*, 4529, 1997.
- Pasko, V. P., U. S. Inan, and T. F. Bell, Spatial structure of sprites, *Geophys. Res. Lett.*, *25*, 2123, 1998a.
- Pasko, V. P., U. S. Inan, and T. F. Bell, Mechanism of ELF radiation from sprites, *Geophys. Res. Lett.*, *25*, 3493, 1998b.
- Reagan, J. B., R. E. Meyerott, R. C. Gunton, et al., Modeling of the ambient and disturbed ionospheric media pertinent to ELF/VLF propagation, in *Medium, Long, and Very Long Wave Propagation (at Frequencies Less Than 3000 kHz)*, edited by J. S. Berlose, pp. 33-1–33-10, AGARD Conference Proceedings No 305, 1981.
- Sentman, D. D., E. M. Wescott, D. L. Osborne, D. L. Hampton, and M. J. Heavner, Preliminary results from the Sprites 94 campaign: Red Sprites, *Geophys. Res. Lett.*, *22*, 1205, 1995.
- Stanley, M., P. Krehbiel, M. Brook, C. Moore, and W. Rison, High speed video of initial sprite development, *Geophys. Res. Lett.*, *26*, 3201, 1999.
- Stenbaek-Nielsen, H. C., D. R. Moudry, E. M. Wescott, D. D. Sentman, and F. T. Sao Sabbas, Sprites and possible mesospheric effects, *Geophys. Res. Lett.*, *27*, 3827, 2000.
- Wait, J. R., and K. P. Spies, Characteristics of the Earth-ionosphere waveguide for VLF radio waves, *Tech. Note 300*, National Bureau of Standards, Boulder, Colo., Dec. 30, 1964.
- Wescott, E. M., H. C. Stenbaek-Nielsen, D. D. Sentman, M. J. Heavner, D. R. Moudry, and F. T. Sao Sabbas, Triangulation of sprites, associated halos and their possible relation to causative lightning and micrometeors, *J. Geophys. Res.*, *106*, 10,467, 2001.

V. P. Pasko, CSSL Laboratory, The Pennsylvania State University, 211 B EE East, University Park, PA 16802-2706, USA. (vpasko@psu.edu)

H. C. Stenbaek-Nielsen Geophysical Institute, University of Alaska Fairbanks, AK 99775, USA. (hnielsen@gi.alaska.edu)